New biorthogonal potential–density basis functions

Alireza Rahmati[1]★ and Mir Abbas Jalali[2,3]★

[1]*Sterrewacht Leiden, Leiden University, PO Box 9513, 2300 RA Leiden, the Netherlands*
[2]*Sharif University of Technology, Azadi Avenue, Tehran, Iran*
[3]*School of Astronomy, Institute for Studies in Theoretical Physics and Mathematics (IPM), PO Box 19395-5531, Tehran, Iran*

ABSTRACT

We use the weighted integral form of spherical Bessel functions and introduce a new analytical set of complete and biorthogonal potential–density basis functions. The potential and density functions of the new set have finite central values and they fall off, respectively, similar to $r^{-(1+l)}$ and $r^{-(4+l)}$ at large radii, where l is the latitudinal quantum number of spherical harmonics. The lowest order term associated with $l = 0$ is the perfect sphere of de Zeeuw. Our basis functions are intrinsically suitable for the modelling of three-dimensional, soft-centred stellar systems and they complement the basis sets of Clutton-Brock, Hernquist & Ostriker and Zhao. We test the performance of our functions by expanding the density and potential profiles of some spherical and oblate galaxy models.

Key words: stellar dynamics – methods: analytical – methods: numerical – celestial mechanics – galaxies: kinematics and dynamics.

1 INTRODUCTION

Solving Poisson's equation is an important step in the study of self-gravitating stellar systems (Binney & Tremaine 2008). Expanding the density distribution and its conjugate potential field in terms of a complete basis set is one of the most efficient methods that investigators have extensively applied to *N*-body simulations (Fridman & Polyachenko 1984; Hernquist & Ostriker 1992; Earn & sellwood 1995; Meza & Zamorano 1997; Buyle et al. 2007; Weinberg & Katz 2007) and to the first-order stability analysis of both flat (Kalnajs 1977; Pichon & Cannon 1997; Jalali & Hunter 2005; Jalali 2007) and three-dimensional galaxies (Saha 1991; Weinberg 1991). Consequently, the success of those studies highly depends on the choice of basis set. Desirable potential and density basis functions should be biorthogonal and converge rapidly in order to decrease the computational noise and cost. Nevertheless, finding a suitable basis set is not an easy task and only few analytical basis sets have been found for three-dimensional stellar systems.

For stellar systems of finite size, spherical Bessel functions are the classical biorthogonal eigenfunctions of the Laplace operator and they have been used in the stability analysis of certain spherical galaxies (Fridman & Polyachenko 1984; Allen, Palmer & Papaloizou 1990; Weinberg 1991). For galaxy models of infinite extent, three biorthogonal potential–density (PD) basis sets have been developed by Clutton-Brock (1973, hereafter CB73), Hernquist & Ostriker (1992, hereafter HO92) and Zhao (1996).

CB73 and HO92 set the lowest order terms of their basis functions to the Plummer (1911) and Hernquist (1990) models while Zhao (1996) uses an α-model with the density

$$\rho(r) = \frac{C}{r^{2-1/\alpha}(1 + r^{1/\alpha})^{2+\alpha}}, \tag{1}$$

where C is a constant parameter. The lowest order term of a PD set does not necessarily need to be spherical (Syer 1995), but an orthonormalization using the standard Gram–Schmidt procedure must be adopted (Saha 1991; Robijn & Earn 1996) to guarantee the completeness of the set.

Apart from the quoted analytic basis functions, numerically generated sets have also become available. Weinberg (1999) assumed the form of the lowest order basis functions and numerically solved the Strum–Liouville equation to obtain biorthogonal basis functions of higher orders. Despite this worthwhile contribution, the propagation of computational noise during the application of numerical basis functions has become problematic in recent *N*-body experiments (Kalapotharakos, Efthymiopoulos & Voglis 2008), which justify the ongoing search for new analytical basis functions.

In this paper, we introduce a new analytical set of biorthogonal PD basis functions whose potential and density components have finite central values, fall off similar to HO92 functions as $r \to \infty$, and their lowest order term is the perfect sphere of de Zeeuw (1985). We derive and evaluate the weighted integral forms of spherical Bessel functions in Section 2, and obtain the radial basis functions in terms of associated Legendre functions. In Section 3, we use the new basis set and generate the series representations of certain spherical and oblate galaxy models. We end this paper with concluding remarks.

★E-mail: rahmati@strw.leidenuniv.nl (AR); mjalali@sharif.edu (MAJ)

2 POTENTIAL–DENSITY PAIRS

We define $\boldsymbol{r} = (r, \theta, \phi)$ as the position vector expressed in terms of usual spherical coordinates, with r, θ and ϕ being the radial distance from the origin, colatitude and azimuthal angle, respectively. We also assume that the mean-field potential and density functions of a stellar system admit the following expansions:

$$\Phi(\boldsymbol{r}) = \sum_{nlm} P_{nlm} \Phi_{nlm}(\boldsymbol{r}), \tag{2a}$$

$$\rho(\boldsymbol{r}) = \sum_{nlm} D_{nlm} \rho_{nlm}(\boldsymbol{r}). \tag{2b}$$

The basis functions $\Phi_{nlm}(\boldsymbol{r})$ and $\rho_{nlm}(\boldsymbol{r})$ satisfy Poisson's equation

$$\nabla^2 \Phi_{nlm}(\boldsymbol{r}) = 4\pi G \rho_{nlm}(\boldsymbol{r}), \tag{3}$$

where n and l are the radial and latitudinal quantum numbers corresponding to r and θ, respectively, and m is the azimuthal Fourier number associated with ϕ. G is the universal constant of gravitation. We proceed with a case that ρ_{nlm} is proportional to Φ_{nlm}. This reduces Poisson's equation to the eigenvalue problem

$$\nabla^2 \Phi_{nlm}(\boldsymbol{r}) = -4\pi G k^2 \Phi_{nlm}(\boldsymbol{r}) \tag{4}$$

that involves the Laplace operator ∇^2 and a constant parameter k. Since the Laplace operator is Hermitian, its associated eigenfunctions form a complete biorthogonal basis set. The coefficients P_{nlm} and D_{nlm} thus become identical. The spherical harmonics $Y_{lm}(\theta, \phi)$ and the spherical Bessel functions $j_n(kr)$ are the classical solutions of (4).

While $Y_{lm}(\theta, \phi)$ show an acceptable performance in the expansion of physical quantities in terms of angle variables, Bessel functions do not look like galactic profiles and cannot generate efficient expansions (Weinberg 1999). We extend the method of Clutton-Brock (1972) to three-dimensional systems and express the eigenfunctions as

$$\Phi_{nlm}(\boldsymbol{r}) = -Y_{lm}(\theta, \phi)\psi_{nl}(r), \tag{5a}$$

$$\rho_{nlm}(\boldsymbol{r}) = Y_{lm}(\theta, \phi)\rho_{nl}(r), \tag{5b}$$

where

$$\psi_{nl}(r) = \int_0^\infty j_l(kr)g_{nl}(k)\,\mathrm{d}k, \tag{6a}$$

$$\rho_{nl}(r) = \frac{1}{4\pi G}\int_0^\infty j_l(kr)g_{nl}(k)k^2\,\mathrm{d}k. \tag{6b}$$

The functions $g_{nl}(k)$ ($n, l = 0, 1, 2, \dots$) are to-be-determined functions that we require to satisfy the biorthogonality condition

$$\int \Phi_{nlm}(\boldsymbol{r})[\rho_{n'l'm'}(\boldsymbol{r})]^* \mathrm{d}\boldsymbol{r} = I_{nlm}\delta_{nn'}\delta_{ll'}\delta_{mm'}. \tag{7}$$

Here, the asterisk denotes complex conjugation and $\delta_{ii'}$ is the Kronecker delta. Substituting from (5) and (6) in (7) and using the identity

$$\int_{-1}^{1} \mathrm{d}(\cos\theta) \int_0^{2\pi} \mathrm{d}\phi\, Y_{lm}(\theta, \phi) Y_{l'm'}^*(\theta, \phi) = \delta_{ll'}\delta_{mm'}, \tag{8}$$

the orthogonality condition (7) reduces to

$$-\frac{1}{4\pi G}\int_0^\infty g_{nl}(k)\mathrm{d}k \int_0^\infty g_{n'l}\left(k'\right) k'^2\,\mathrm{d}k'$$
$$\times \int_0^\infty j_l(kr)j_l\left(k'r\right) r^2\mathrm{d}r = I_{nlm}\delta_{nn'}. \tag{9}$$

The innermost integral on the left-hand side of (9) is evaluated according to the Fourier–Bessel theorem (Ugincius 1972) as

$$\int_0^\infty j_l(kr)j_l(k'r)r^2\,\mathrm{d}r = \frac{\pi}{2k^2}\delta(k'-k), \tag{10}$$

with $\delta(k'-k)$ being the Dirac delta function. Substituting (10) in (9) leads to

$$-\frac{1}{8G}\int_0^\infty g_{nl}(k)g_{n'l}(k)\,\mathrm{d}k = \overline{I}_{nl}\delta_{nn'} \equiv I_{nlm}\delta_{nn'}. \tag{11}$$

This condition requires $g_{nl}(k)$ to be any orthogonal set of functions over the semi-infinite k-domain. Our special choice is $g_{nl}(k) = k^l L_n^p(2k)e^{-k}$, where $L_q^p(k)$ are the associated Laguerre polynomials that obey the following orthogonality relation:

$$\int_0^\infty e^{-k}k^p L_q^p(k)L_{q'}^p(k)\,\mathrm{d}k = \frac{(q+p)!}{q!}\delta_{qq'}. \tag{12}$$

Consequently, the constant parameters on the right-hand side of equation (11) become

$$\overline{I}_{nl} = -\frac{(n+2l)!}{G2^{2l+4}n!}, \tag{13}$$

and our radial basis functions read

$$\psi_{nl}(r) = \int_0^\infty j_l(kr)L_n^{2l}(2k)e^{-k}k^l\,\mathrm{d}k, \tag{14a}$$

$$\rho_{nl}(r) = \frac{1}{4\pi G}\int_0^\infty j_l(kr)L_n^{2l}(2k)e^{-k}k^{l+2}\,\mathrm{d}k. \tag{14b}$$

The integrals in (14) converge rapidly, which makes their evaluation a straightforward task by numerical methods. However, closed-form analytical expressions can also be derived for $\psi_{nl}(r)$ and $\rho_{nl}(r)$ as we explain below. We utilize the series form of the Laguerre functions

$$L_n^{2l}(2k) = \sum_{i=0}^n (-1)^i \binom{n+2l}{n-i}\frac{(2k)^i}{i!}, \tag{15}$$

and express $j_l(kr)$ in terms of Bessel functions to rewrite (14b) in the form

$$\rho_{nl}(r) = \frac{1}{4\pi G}\sum_{i=0}^n (-2)^i \binom{n+2l}{n-i}\sqrt{\frac{\pi}{2r}}\frac{1}{i!}$$
$$\times \int_0^\infty J_{l+\frac{1}{2}}(kr)e^{-k}k^{l+i+3/2}\,\mathrm{d}k. \tag{16}$$

Carrying out a change of independent variable as $kr \to u$, transforms equation (16) to

$$\rho_{nl}(r) = \frac{1}{4\pi G}\sum_{i=0}^n (-2)^i \binom{n+2l}{n-i}\sqrt{\frac{\pi}{2}}\frac{r^{-l-i-3}}{i!}$$
$$\times \int_0^\infty J_{l+\frac{1}{2}}(u)e^{-u/r}u^{l+i+3/2}\,\mathrm{d}u. \tag{17}$$

The integral in (17) can be calculated using equation (6.621) in Gradshteyn & Ryzhik (2000). Defining $\xi = 1/\sqrt{1+r^2}$, $\nu_1 = l + i + 3$, $\nu_2 = l + i + 3/2$ and $\mu = -1/2 - l$, we obtain

$$\rho_{nl}(r) = \frac{1}{4\sqrt{2\pi}G}\sum_{i=0}^n \frac{(2l+i+2)(2l+i+1)(n+2l)!}{i!(n-i)!}$$
$$\times (-2)^i \xi^{\nu_1}(1-\xi^2)^{-1/4}P_{\nu_2}^\mu(\xi), \tag{18}$$

where $P_\nu^\mu(x)$ are associated Legendre functions. Following a similar procedure, one can show that

$$\psi_{nl}(r) = \sqrt{\frac{\pi}{2}}\sum_{i=0}^n \frac{(n+2l)!}{i!(n-i)!}(-2)^i \xi^{\nu_3}(1-\xi^2)^{-1/4}P_{\nu_4}^\mu(\xi), \tag{19}$$

where $\nu_3 = l + i + 1$ and $\nu_4 = l + i - 1/2$. The associated Legendre functions can be determined through the recursive relations (Gradshteyn & Ryzhik 2000):

$$(\nu - \mu + 1)P^{\mu}_{\nu+1}(\xi) + (\nu + \mu)P^{\mu}_{\nu-1}(\xi) = (2\nu + 1)\xi P^{\mu}_{\nu}(\xi), \quad (20a)$$

$$P^{\mu}_{\nu-1}(\xi) - P^{\mu}_{\nu+1}(\xi) = (2\nu + 1)(1 - \xi^2)^{1/2} P^{\mu-1}_{\nu}(\xi), \quad (20b)$$

which start from

$$P^{-1/2}_{\nu}(\xi) = \sqrt{\frac{2}{\pi \sin \beta}} \frac{\sin [(\nu + 1/2)\beta]}{(\nu + 1/2)}, \quad \cos \beta = \xi. \quad (21)$$

The lowest order members of our PD family are

$$\psi_{00}(r) = -\frac{1}{r} \arctan r, \quad (22a)$$

$$\rho_{00}(r) = \frac{1}{2\pi G} \frac{1}{(1 + r^2)^2}, \quad (22b)$$

which define the perfect sphere of de Zeeuw (1985). We have therefore found a biorthogonal basis set that is distinct from CB73, HO92 and Zhao's (1996) functions. Moreover, from (21) and the recursive relations (20), we deduce that the functions $P^{\mu}_{\nu_4}(\xi)$ and $P^{\mu}_{\nu_2}(\xi)$ behave, respectively, similar to r^0 and r^{-1} in the limit of $r \to \infty$. It can thus be verified that $\psi_{nl}(r) \sim r^{-(1+l)}$ and $\rho_{nl}(r) \sim r^{-(4+l)}$ hold at large radii. The potential functions of CB73, HO92 and ours have finite central values and they fall off similar to $r^{-(1+l)}$ at large radii. Our density functions are analytic at the galactic centre as are the functions of CB73, but they behave like HO92 functions in the limit of $r \to \infty$. The best performance of our basis set is thus expected in soft-centred systems whose outer density profiles are similar to r^{-4}.

In Fig. 1, we have displayed several members of our basis functions for $l = 0, 2$. At the centre, both the potential and density functions have finite, non-zero values for $l = 0$, and they vanish there for $l \neq 0$. The expected yet interesting property of $\psi_{nl}(r)$ and $\rho_{nl}(r)$ is their oscillatory nature. The number of peaks of our functions (in the radial direction) is equal to $n + 1$. Our numerical experiments show that the series built by oscillatory functions have a faster and more accurate mean convergence as compared to functions that do not share this feature.

Our functions have a length-scale that has been set to unity so far. In general, changing the length-scale is necessary to reconstruct galaxies of different core radii. A scaling parameter r_0 can be easily introduced to our formulation by replacing $g_{nl}(k)$ with $g_{nl}(kr_0)$ (Clutton-Brock 1972). This implies the following transformations:

$$\Phi_{nlm}(r, \theta, \phi) \to r_0^{-1}\Phi_{nlm}(r/r_0, \theta, \phi), \quad (23a)$$

$$\rho_{nlm}(r, \theta, \phi) \to r_0^{-3}\rho_{nlm}(r/r_0, \theta, \phi), \quad (23b)$$

$$\overline{I}_{nl} \to r_0^{-1}\overline{I}_{nl}. \quad (23c)$$

3 RECONSTRUCTION OF MODEL GALAXIES

Biorthogonal basis functions, similar to ours, have the advantage that the coefficients $P_{nlm} = D_{nlm}$ in (2) can be determined using either the potential $\Phi(\mathbf{r})$ or the density $\rho(\mathbf{r})$ through the following formulae:

$$P_{nlm} \equiv D_{nlm} = \frac{1}{\overline{I}_{nl}} \int \rho(\mathbf{r})[\Phi_{nlm}(\mathbf{r})]^* \, d\mathbf{r}$$

$$= \frac{1}{\overline{I}_{nl}} \int \Phi(\mathbf{r})[\rho_{nlm}(\mathbf{r})]^* \, d\mathbf{r}, \quad (24)$$

where we have used the orthogonality conditions (7) and (11). In what follows, we examine the performance of our basis functions by
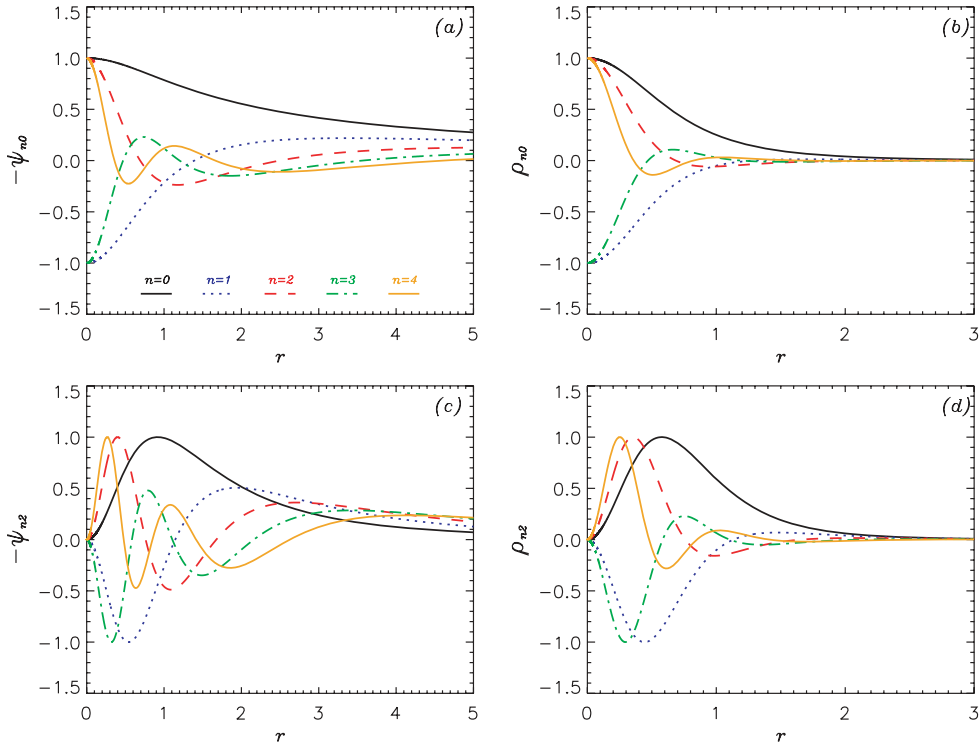

Figure 1. Left-hand panels display the radial parts of the potential basis functions, $\psi_{nl}(r)$, for $n = 0, 1, 2, 3, 4$, and right-hand panels show their conjugate density functions $\rho_{nl}(r)$. Top and bottom panels correspond to $l = 0$ and 2, respectively. All functions have been normalized to their maximum values.

the series reconstruction of the density profiles and potential fields of some model galaxies.

3.1 Spherical models

We followed the standard procedure of using spherical harmonics for the expansions of physical quantities in terms of angular variables and introduced a new set of radial basis functions. So we need to examine the performance of our radial set by reproducing some spherical models. As case studies, we choose the isochrone and Plummer models of total mass M and length-scale b (Binney & Tremaine 2008). Our basis functions have finite values at the centre, and it would be interesting to learn whether they are suitable for the reconstruction of models with central density cusps. For doing so, we also analyse the performance of our basis functions by applying them to Dehnen's γ models (Dehnen 1993). The density profiles of Dehnen's models diverge similar to $r^{-\gamma}$ in central regions and fall off proportional to r^{-4} at large radii. Dehnen's models also have a length-scale b. The model with $\gamma = 0$ has an intrinsic core at the centre, and for $\gamma = 3/2$ a central cusp with an intermediate slope between Hernquist (1990) and Jaffe (1983) models is created. In our study, we choose two models with $\gamma = 1/2$ and $3/2$.

We have set $r_0 = 1$ and used equation (24) to compute the coefficients of expansion D_{nlm} for the Plummer, isochrone and Dehnen models. The parameters of the isochrone model have been set to $GM = 1$ and $b = 0.5$. For other models, we have used $GM = 1$ and $b = 1$. Our results are displayed in Fig. 2, which shows how $|D_{n00}|$ vary versus n. We note that all coefficients with $l, m \neq 0$ vanish because of the spherical symmetry. It is evident that $|D_{n00}|$ decrease several orders of magnitude by including more terms in the series expansions. Although for $\gamma = 1/2$ the coefficients of Dehnen's model fall off similar to other soft-centred models, they decay mildly for $\gamma = 3/2$. This shows very slow and unfavourable convergence of our series expansion in steeper cusps as is expected.

Having expansion coefficients, the original model can be constructed using (2). Denoting the original PD pair by $[\Phi_0(r), \rho_0(r)]$ and their series representations by $[\Phi(r), \rho(r)]$, we compute the relative errors $E_\rho = (\rho - \rho_0)/\rho_0$ and $E_\Phi = (\Phi - \Phi_0)/\Phi_0$ and their absolute magnitudes $\delta_\rho = |E_\rho|$ and $\delta_\Phi = |E_\Phi|$ to measure the performance of the basis set. We have used the first 10 radial basis elements ($n_{max} = 9$) to compute $[\Phi(r), \rho(r)]$. The results are shown in Fig. 3. It is seen that δ_Φ is below 2 per cent in all parts of the Plummer, isochrone and Dehnen's $\gamma = 1/2$ models, and also for
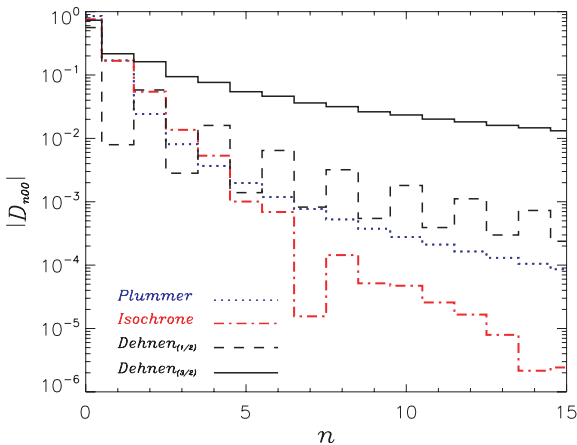

Figure 2. The absolute magnitudes $|D_{n00}|$ of the expansion coefficients versus the radial quantum number n for several spherical models.

$r > 0.1$ in Dehnen's $\gamma = 3/2$ model. The reason is the similarity of $\psi_{n0}(r)$ defined in (19) to the potential profiles of the chosen models. The large error magnitude near the centre of Dehnen's $\gamma = 3/2$ model is due to its sharper density cusp that prohibits a simultaneous convergence of the density and potential series.

The reconstruction of $\rho_0(r)$, however, has not been successful in Dehnen's $\gamma = 3/2$ model because of its sharper cusp. Large values of δ_ρ are also observed in the central part of Dehnen's $\gamma = 1/2$ model (due to its cuspy nature), and at large radii of the Plummer model due to its rapid density falloff, which is steeper than our $\rho_{n0}(r) \sim r^{-4}$. The isochrone model is the only case that has been reproduced with a reliable accuracy in all parts of the galaxy. In fact, the isochrone model shares two basic features of our new basis set: (i) it has a soft core and (ii) its outer potential and density profiles decay, respectively, similar to r^{-1} and r^{-4} as do the envelopes of the functions $\psi_{n0}(r)$ and $\rho_{n0}(r)$. In Fig. 3(a), for $n_{max} = 9$ the magnitude of δ_ρ is less than 1 per cent over the range $0 \leq r \lesssim 20$ and it saturates at a level of $\delta_\rho \approx 5$ per cent for $r > 20$. By increasing n_{max} to 14, both δ_ρ and δ_Φ remain smaller than 1 per cent over the range $0 < r < 100$. This result can also be deduced from Fig. 2 that shows a monotonic decay for $|D_{n00}|$ versus n.

In general, the density error δ_ρ is larger than δ_Φ. We explain this by calculating E_ρ in terms of E_Φ and its derivatives. The original potential and density functions satisfy Poisson's equation, and since our basis functions are biorthogonal, the relation $\nabla^2 \Phi = 4\pi G\rho$ also holds between the expanded quantities. We can therefore write

$$\nabla^2 (\Phi - \Phi_0) = 4\pi G (\rho - \rho_0), \qquad (25)$$

which is divided by ρ_0 to obtain

$$\frac{1}{\rho_0} \nabla^2 (\Phi - \Phi_0) \equiv \frac{1}{\rho_0} \nabla^2 (\Phi_0 E_\Phi) = 4\pi G E_\rho. \qquad (26)$$

For the Laplace operator with spherical symmetry, equation (26) leads to

$$\frac{1}{\rho_0} \left[\Phi_0 \nabla^2 E_\Phi + E_\Phi \nabla^2 \Phi_0 + 2 \frac{d\Phi_0}{dr} \frac{dE_\Phi}{dr} \right] = 4\pi G E_\rho. \qquad (27)$$

Substituting $4\pi G\rho_0$ for $\nabla^2 \Phi_0$ in (27) yields

$$\frac{\Phi_0}{\rho_0} \nabla^2 E_\Phi + 4\pi G E_\Phi + \frac{2}{\rho_0} \frac{d\Phi_0}{dr} \frac{dE_\Phi}{dr} = 4\pi G E_\rho. \qquad (28)$$

We are interested in the local extrema of E_Φ. There are n_{max} number of such points whose existence is deduced from the oscillatory nature of basis functions. The derivative dE_Φ/dr vanishes at the extrema of E_Φ, and equation (28) reads as

$$\frac{E_\rho}{E_\Phi} = 1 + \frac{\Phi_0}{4\pi G\rho_0} \frac{1}{E_\Phi} \frac{d^2 E_\Phi}{dr^2}. \qquad (29)$$

This is a useful relation that gives a credible estimate of E_ρ/E_Φ based on the quotient Φ_0/ρ_0 and the curvature of E_Φ. For each model, we have independently computed δ_ρ from (29) and have plotted the results (scattered squares in Fig. 3) against the numerical graph of δ_ρ obtained from the series expansion of $\rho_0(r)$. There is a close agreement between the results of the two methods, confirming the fact that the drift $\delta_\rho - \delta_\Phi$ is independent of the choice of basis set and it persists in any series solution of Poisson's equation.

Neither the isochrone nor Dehnen's $\gamma = 1/2$ models match the zeroth-order terms of CB73, HO92 and our basis functions. Therefore, the performance of these basis sets can be fairly compared by expanding the isochrone and Dehnen's $\gamma = 1/2$ models (Fig. 4). It is seen that CB73 functions have a poor performance in reproducing both models. Our functions have performed better than HO92 functions for $r \lesssim 1$ in the isochrone model. Nevertheless, HO92
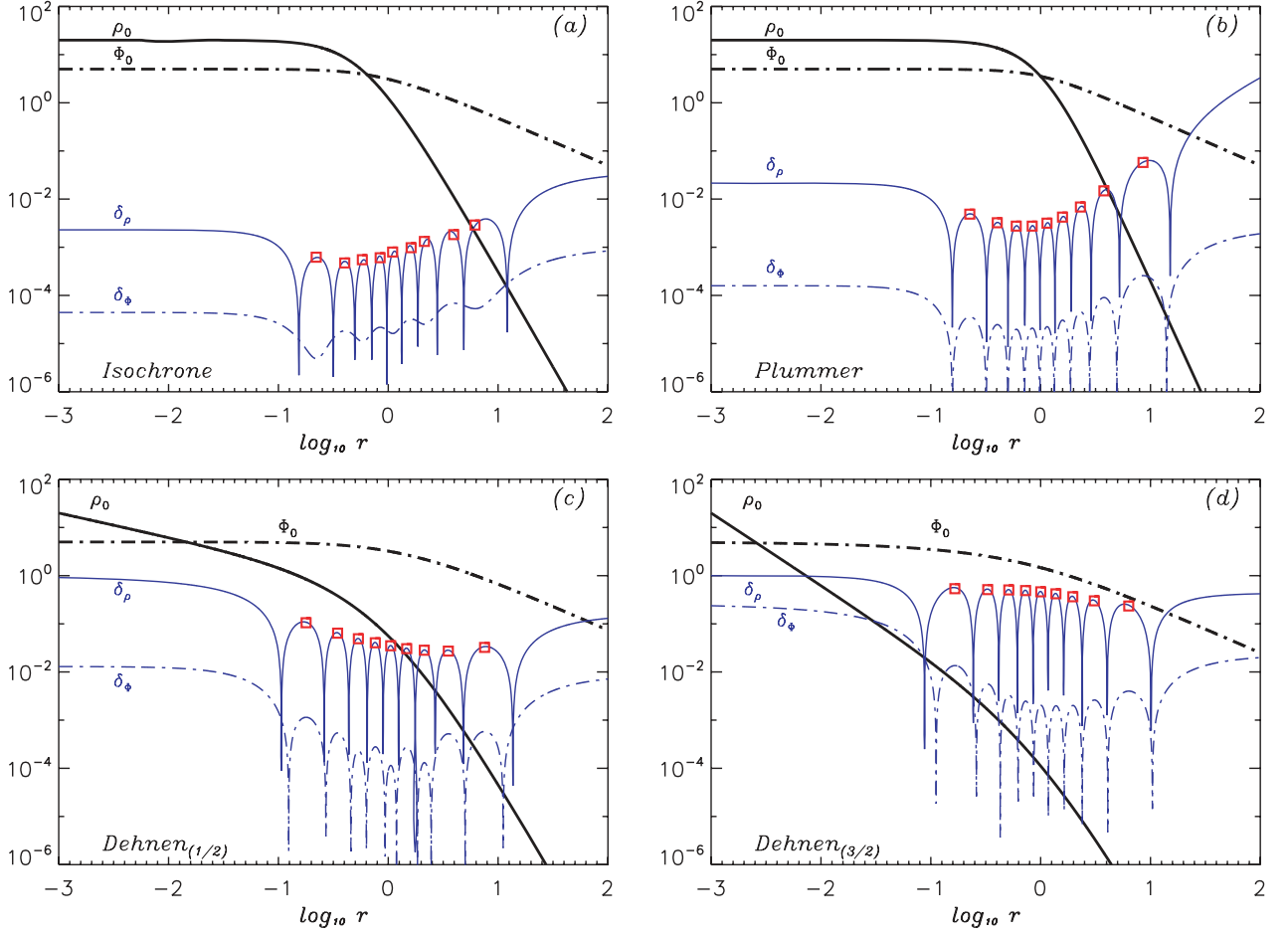
Figure 3. The relative errors δ_ρ (thin solid lines) and δ_Φ (thin dash-dotted lines) in the series reconstruction of the density ρ_0 (thick solid lines) and the absolute magnitude of its associated potential Φ_0 (thick dash-dotted lines). The basis functions are those of equations (18) and (19). Panels *a*, *b*, *c* and *d* correspond, respectively, to the isochrone, Plummer, Dehnen's $\gamma = 1/2$ and Dehnen's $\gamma = 3/2$ models. The functions $\Phi(r)$ and $\rho(r)$ have been computed by taking the first 10 basis functions ($n_{max} = 9$). In each error curve, there are $n_{max} + 1$ sharp minima that correspond to the locations of exact match between the original functions and their series representations. The scattered squares show the magnitude of δ_ρ calculated from equation (29). The central values of Φ_0 and ρ_0 have been normalized to some arbitrary numbers just for the purpose of visualizing their profiles against the error curves.
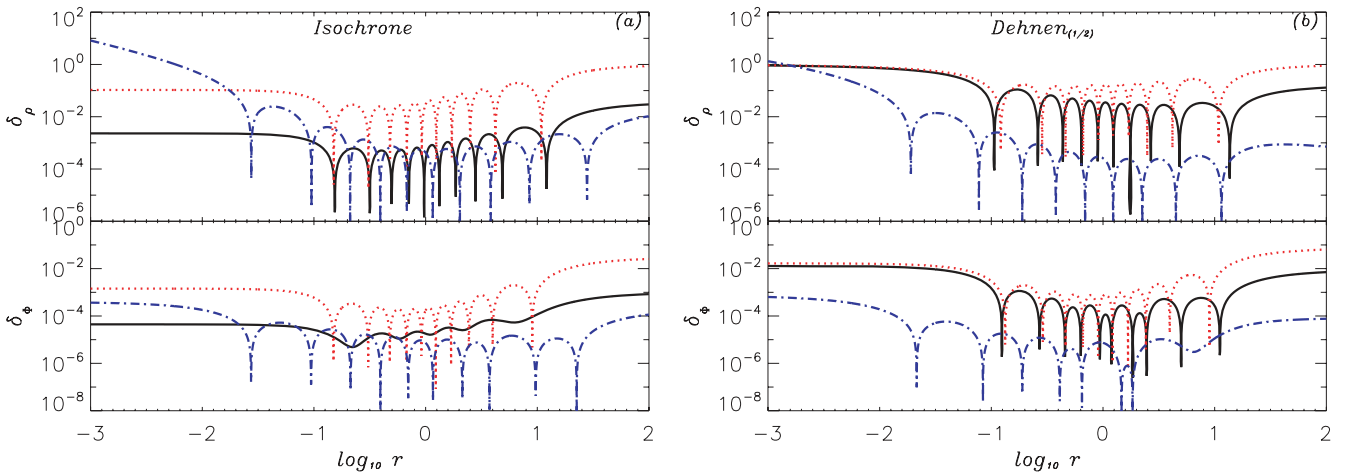

Figure 4. Variations of δ_ρ (top panels) and δ_Φ (bottom panels) for the isochrone (left-hand panels) and Dehnen's $\gamma = 1/2$ (right-hand panels) models. Solid, dotted and dash-dotted lines, respectively, correspond to the expansions by our, CB73 and HO92 basis functions. The length-scale of the isochrone model is $b = 0.5$ and that of Dehnen's $\gamma = 1/2$ model is $b = 1$. For both models, we have set $GM = 1$ and all basis functions have the length-scale of $r_0 = 1$.

functions have resulted in the lowest magnitudes of δ_Φ and δ_ρ for $r \gtrsim 1$ in the isochrone model and for $r \gtrsim 0.005$ in Dehnen's $\gamma = 1/2$ model. Our results show that the envelopes of basis functions *must follow* the radial profiles of both the density and the potential functions of a spherical stellar system to assure a reliable expansion. Dehnen's shallow density cusp cannot be reproduced even by cuspy set of HO92 (see Fig. 4b) because the central envelope of HO92's density functions is proportional to r^{-1}, while Dehnen's density profile diverges as $r^{-1/2}$.

3.2 Oblate galaxy models

The modelling of oblate galaxy models is a bigger challenge because the series of radial basis functions must converge together with spherical harmonics. It is therefore hard to predict how the combination of radial and angular functions will behave. As our case studies of spheroidal galaxy models, we choose an oblate Kuzmin & Kutuzov (1962) model and a perfect spheroid (de Zeeuw 1985), and reproduce their density distributions using the series of CB73, HO92 and our new biorthogonal sets. In the spherical limit, the Kuzmin–Kutuzov model reduces to Hénon's (1959) isochrone and the perfect spheroid becomes the perfect sphere, which is the lowest order term of our new basis set. Since our functions showed slow convergence for Dehnen's spherical models near the centre (see Figs 2 and 3), we did not extend our analysis to their flattened (Dehnen & Gerhard 1994) counterparts. Moreover, we proved in Section 3.1 that the potential expansions are always more accurate than the density ones. This applies to oblate models as well, and therefore, we confine ourselves to computing δ_ρ.

Defining $u^2 = a^2 c^2 + c^2 R^2 + a^2 z^2$, the density functions of the Kuzmin–Kutuzov and perfect spheroidal models are, respectively, given by (de Zeeuw 1985; Dejonghe & de Zeeuw 1988)

$$\rho_{KK}(R, z) = \frac{Mc^2}{4\pi} \frac{(a^2 - c^2)R^2 + a^4 + 2u^2 + 3a^2 u}{u^3 \left(R^2 + z^2 + a^2 + c^2 + 2u\right)^{3/2}}, \tag{30a}$$

$$\rho_{PS}(R, z) = \frac{M}{\pi^2 \sqrt{1 - e^2}} \left(1 + R^2 + \frac{z^2}{1 - e^2}\right)^{-2}, \tag{30b}$$

where $R = r \sin \theta$ and $z = r \cos \theta$, and z is the symmetry axis. The parameter e is the flattening of the perfect spheroidal model.

The Kuzmin–Kutuzov model has equipotential surfaces of the axis ratio $\sqrt{c/a}$ near the centre, and we choose its length-scale so that $a + c = 1$. Here, again, M is the total mass of the galaxy.

The isocontours of the original and expanded density functions are displayed in Fig. 5 for a perfect spheroidal model of $e = 0.5$ and for a Kuzmin–Kutuzov model of $c/a = 0.5$. We have set $r_0 = 1$ and $n_{max} = 9$, and used $l_{max} = 8$ for the Kuzmin–Kutuzov model and $l_{max} = 4$ for the perfect spheroid, respectively. The maximum deviation from the original model occurs near the R-axis because of the slow convergence of spherical harmonics as $\theta \to \pi/2$. Therefore, we have shown in Fig. 6 the variation of δ_ρ versus R in the equatorial plane. Note that the existence of a symmetry axis implies $D_{nlm} = 0$ for odd latitudinal quantum numbers and for $m \neq 0$.

Our experiments show that by increasing l_{max} the density expansion near the equatorial plane is improved. It is evident that HO92 functions have failed in reproducing the finite central densities of both models but they have best fitted the outer parts. For $R \gtrsim 0.2$, the error indicator δ_ρ is smaller for HO92 functions than CB73 ones by almost 1 order of magnitude, and that of our new functions lies between them. Nonetheless, only our functions result in a very small error level of ≤ 1 per cent for $R \lesssim 0.2$ in both the models. This shows that our new basis set is the most trusted tool for modelling all parts of cored, oblate galaxies whose outer potential and density profiles fall off similar to r^{-1} and r^{-4}, respectively. We note that the magnitude of δ_ρ rises substantially and then saturates beyond the radial distance $R \approx 10$ where the density has fallen to 0.1 per cent of its central value. This property is shared by all tested basis sets. It is by increasing the number of radial basis functions (n_{max}) together with the precision of computations that the error magnitude is suppressed at large radii.

It is helpful to compare our results with Robijn & Earn (1996) who have designed a set of basis functions for the perfect spheroidal models. Their functions have been orthonormalized using the Gram–Schmidt procedure. For $n_{max} = 9$ and $l_{max} = 4$ that match the number of series terms in our setup, they reported a maximum error of $\delta_\rho \approx 30$ per cent in the density expansion for a perfect spheroid of ellipticity $e = 0.5$ and inside the domain $0 < R, z < 2$. In the same region, our density expansion leads to a maximum error of $\delta_\rho \approx 7$ per cent, which is notably small.
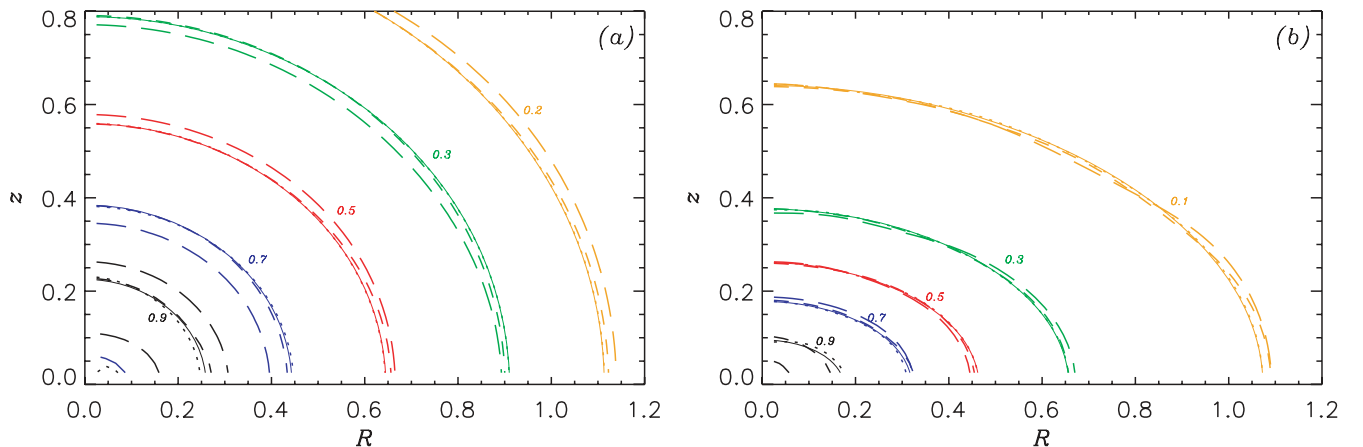

Figure 5. Left-hand panel: density isocontours of a perfect spheroid. Solid lines correspond to the exact model density and short-dashed, long-dashed and dotted curves are associated with density expansions using our, CB73 and HO92 basis functions, respectively. The ellipticity of the model is $e = 0.5$. Right-hand panel: same as the left-hand panel but for an oblate Kuzmin–Kutuzov model with $c/a = 0.5$. In both figures, the levels of isocontours indicate the fraction of maximum density.
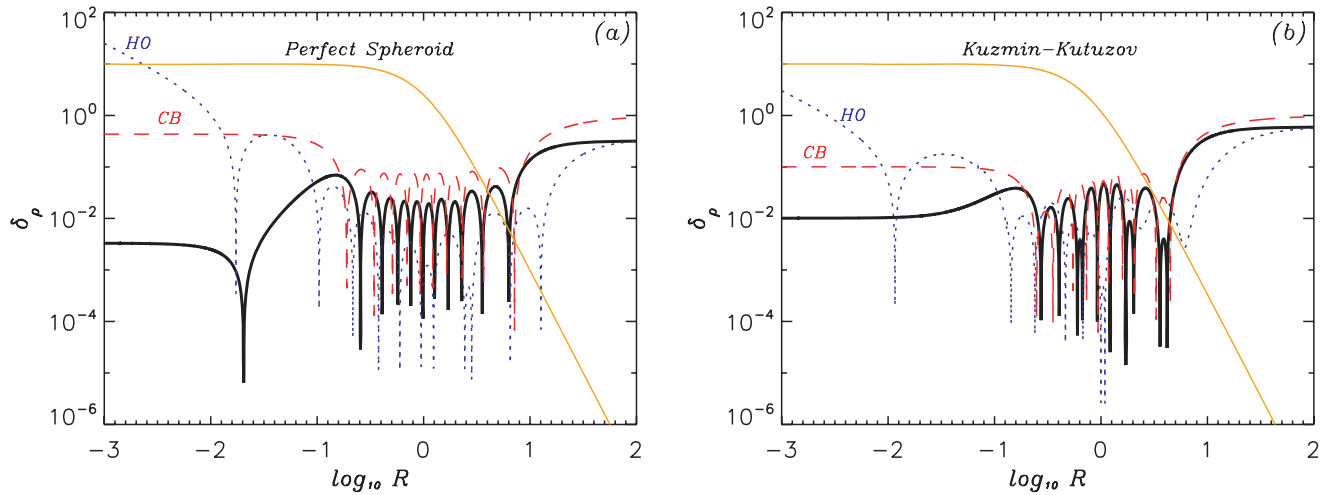
Figure 6. Radial variation of the relative error δ_ρ (oscillatory curves) against the model density on the equatorial plane ($z = 0$) of the same prefect spheroid (panel *a*) and Kuzmin–Kutuzov (panel *b*) models of Fig. 5. Dashed, dotted and thick solid curves correspond, respectively, to CB73, HO92 and our basis functions.

4 CONCLUSION

The lack of suitable PD basis sets is a serious problem in dynamical studies that solve Poisson's equation using the series expansions. For three-dimensional stellar systems, only few analytic basis sets have been found and most researchers have tailored numerical functions to cope with their specific problems. In this paper, we generalized Clutton-Brock's (1972) idea to three-dimensional systems and introduced a new set of basis functions, which have the useful property of biorthogonality. Our functions complement the CB73, HO92 and Zhao's (1996) basis sets because neither of them exhibits the following properties together: (i) a finite central density and (ii) an outer density falloff similar to r^{-4}. For instance, the integrable models of de Zeeuw (1985) and their perturbed states can be efficiently expanded by our basis functions. Thus, we get one step closer to the stability analysis of elliptical galaxies whose potentials are of the Stäckel form. Robijn (1995) and Sellwood & Valluri (1997) investigated the instabilities of some spheroidal galaxy models but calculating the eigenspectra of more general triaxial systems remains as a big challenge.

Our functions were derived in terms of elementary rational, and associated Legendre functions for which recursive formulae are available. We carried out a mathematical error analysis and then compared its results by numerical experiments to show that density expansions converge slower than the potential ones. By expanding several spherical and oblate galaxy models, we showed that an improper choice of basis functions can contribute potentially dangerous errors to dynamical studies. Not only the nature of the galactic centre (cuspy or cored) is an important factor for the selection of basis functions, but the outer density and potential profiles also matter. Neither our new set nor other basis functions cited in this paper are suitable for the modelling of cuspy dark matter haloes whose density profiles decay outwards like r^{-3}. It is possible to find basis sets compatible with such systems, but that will require other choices of the weighting functions $g_{nl}(r)$ that must be orthogonal over the r-domain in three dimensions. It is remarked that we had set the length-scale of our basis functions to $r_0 = 1$ in all of our case studies, but there is always an optimum value of r_0 that gives the best fit. For example, the isochrone model is best fitted by setting $r_0 = 2b$. We therefore recommend an optimal search for finding the best minimizer of δ_Φ.

REFERENCES

Allen A. J., Palmer P. L., Papaloizou J., 1990, MNRAS, 242, 576
Binney J., Tremaine S., 2008, Galactic Dynamics, 2nd edn. Princeton Univ. Press, Princeton, NJ
Buyle P., van Hese E., de Rijcke S., Dejonghe H., 2007, 375, 1157
Clutton-Brock M., 1972, Ap&SS, 16, 101
Clutton-Brock M., 1973, Ap&SS, 23, 55 (CB73)
Dehnen W., 1993, MNRAS, 265, 250
Dehnen W., Gerhard O. E., 1994, MNRAS, 268, 1019
Dejonghe H., de Zeeuw P. T., 1988, ApJ, 333, 90
de Zeeuw P. T., 1985, MNRAS, 216, 273
Earn D. J. D., Sellwood J. A., 1995, ApJ, 451, 533
Fridman A. M., Polyachenko V. L., 1984, Physics of Gravitating Systems., Vol. 2, Springer, New York
Gradshteyn I. S., Ryzhik I. M., 2000, Table of Integrals, Series and Products, 6th edn. Academic Press, London
Hénon M., 1959, Ann. d'Ap., 22, 126
Hernquist L., 1990, ApJ, 356, 359
Hernquist L., Ostriker J. P., 1992, ApJ, 386, 375 (HO92)
Jaffe W., 1983, MNRAS, 202, 995
Jalali M. A., 2007, ApJ, 669, 218
Jalali M. A., Hunter C., 2005, ApJ, 630, 804
Kalapotharakos C., Efthymiopoulos C., Voglis N., 2008, MNRAS, 383, 971
Kalnajs A. J., 1977, ApJ, 212, 637
Kuzmin G. G., Kutuzov S. A., 1962, Bull. Abastumani Ap. Obs., 27, 82
Meza A., Zamorano N., 1997, ApJ, 490, 136
Pichon C., Cannon R. C., 1997, MNRAS, 291, 616
Plummer H. C., 1911, MNRAS, 71, 460
Robijn F. H. A., 1995, PhD thesis, Leiden Observatory. Leiden, the Netherlands

Robijn F. H. A., Earn D. J. D., 1996, MNRAS, 282, 1129
Saha P., 1991, MNRAS, 248, 494
Sellwood J. A., Valluri M., 1997, MNRAS, 287, 124
Syer D., 1995, MNRAS, 276, 1009
Weinberg M. D., 1991, ApJ, 368, 66

Weinberg M. D., 1999, ApJ, 117, 629
Weinberg M. D., Katz N., 2007, MNRAS, 375, 460
Zhao H. S., 1996, MNRAS, 278, 488

This paper has been typeset from a TEX/LATEX file prepared by the author.